Photoionization of semiconductor impurities in the presence of a static electric field

Guy Lamouche and Yves Lépine
Département de Physique et Groupe de Recherche en Physique et Technologie des Couches Minces, Université de Montréal, Case Postale 6128, Succursale "A," Montréal, Québec Canada H3C 3J7
(Received 7 October 1993; revised manuscript received 1 February 1994)

The effect of a static uniform electric field on the photoionization process of an isolated impurity in a semiconductor is studied. The impurity potential is treated with the quantum-defect approach. The limiting hydrogenic and Lucovsky models are also considered. The photoionization process is analyzed with the Fermi's golden rule in the dipolar approximation. We show that the main effects of the static electric field are similar to the Franz-Keldysh effects well known for the photon-induced interband transition: the appearance of a redshift of the lower absorption edge and of an oscillation pattern superimposed on the zero-field photoionization cross section for higher energies. These oscillations are much stronger when the electric-field polarization of the photons is parallel to the static electric field than when it is perpendicular.

I. INTRODUCTION

In this paper, we investigate the photoionization process of an isolated impurity in a semiconductor in the presence of a static, uniform electric field. Photoionization cross-section measurements give useful information on impurity states: energy, nature of the defect, symmetry, electron-phonon coupling, temperature dependence, etc.[1] Our study is motivated by the experimental conditions found in some techniques used to obtain these cross sections. For example, the deep-level optical spectroscopy[2] (DLOS) involves impurities in the depletion region of a junction where the electric field can have an appreciable magnitude. One can question the effect of this electric field on the optical measurements. In the case of a thermal characterization technique like the deep-level transient spectroscopy, such a static field is known to lead to an often non-negligible Poole-Frenkel effect.[3]

Very few papers discuss the effects of a static electric field on the photoionization process of an isolated impurity. Monemar and Samuelson present an experimental curve showing that the electric field indeed affects photoionization measurements by inducing a redshift of the lower absorption edge.[4] On the theoretical side, Coon and Karunasiri look at the problem in the weak field limit.[5] In their work, they use the quantum-defect approach to model the impurity potential. They use the Coulomb Green's function and the WKB approximation in order to obtain the wave function of photoexcited electrons. The photoionization cross section is obtained from this wave function. Their results are valid for weak static electric fields and for photon energies well below the ionization energy of the impurity.

We address the same problem with a simple approach valid for all photon energies. Our treatment is valid for electric fields such that the field ionization processes can be neglected. We consider the photon-induced transition of an electron (hole) from a donor (acceptor) impurity to the conduction (valence) band.[6] The impurity potential is modeled with the quantum-defect approach. We also consider the hydrogenic and Lucovsky limits. The dipolar optical transitions are treated with the Fermi's golden rule.

In Sec. II we give the Hamiltonian of the impurity potential in the presence of a static electric field and describe its eigenstates. In Sec. III we develop an expression for the photoionization cross section starting from the Fermi's golden rule. Asymptotic expressions are discussed in Sec. IV. Calculated photoionization cross sections are finally presented in Sec. V. The details of the calculations for the photoionization cross section and its asymptotic limits are presented in Appendixes A and B.

II. HAMILTONIAN AND EIGENSTATES

In this section, we introduce the Hamiltonian of the impurity potential in presence of a static electric field. We discuss the initial and final states of the photoionization process. For briefness, we consider only the case of a donor impurity. The following treatment can be easily adapted to an acceptor.

A. Quantum-defect Hamiltonian

The charged defect is described using the quantum-defect approach.[7] This model is well discussed in the context of semiconductor impurity photoionization in Refs. 6, 8, and 9. We also consider the limiting hydrogenic[10] (no short-range potential) and Lucovsky[11] (no Coulombic potential) models.

We use a simple form of the effective-mass approximation: a nondegenerate parabolic band with a single extremum. In the following, we denote by $F_n(\vec{r})$ the envelope function of state n with energy E_n. In presence of a static electric field E_{el} heading in the z direction, the

quantum-defect envelope functions $F_n(\vec{r})$ are the solution of the following effective Schrödinger equation:

$$H(\vec{r})F_n(\vec{r}) = \left(-\nabla^2 - \frac{2}{r} + \tilde{V}_{sr}(r) + \gamma z\right)F_n(\vec{r}) = E_n F_n(\vec{r}) \ . \quad (1)$$

The preceding equation is written with lengths and energies given in units of the effective Bohr radius a_0^* and of the effective Rydberg Ry*, respectively. Those quantities are defined as in the hydrogenic effective-mass theory formulation:[10]

$$a_0^* = \frac{\hbar^2 \epsilon}{m^* e^2} \ , \quad \mathrm{Ry}^* = \frac{\hbar^2}{2 m^* a_0^{*2}} \ , \quad (2)$$

where m^* represents the band mass and ϵ the static dielectric constant of the semiconductor. In Eq. (1), $\tilde{V}_{sr}(r)$ is the dimensionless short-range potential associated with the quantum-defect theory and $+\gamma z$ is the static electric-field contribution. The parameter $\gamma = e E_{el} a_0^*/\mathrm{Ry}^*$ represents the energy increase of an electron accelerated by the electric field over a distance equal to the effective Bohr radius (a_0^*) (this energy is written in Ry* units). We use γ in the following to represent the static electric field.

B. Ground state

For the ground-state evaluation, we neglect the field ionization process. The critical field magnitude for the classical field ionization can easily be evaluated if one neglects the ground-state energy shift (Stark shift).[12] In the quantum-defect context, its value is

$$\gamma_c = E_d^2/8 \ = -\frac{1}{8\nu^4}, \quad (3)$$

where $E_d(= -1/\nu^2)$ is the ground state energy of the defect and ν is the quantum-defect parameter. We use this γ_c value as a reference in the following: it gives an upper bound for the electric field. We consider that the lifetime associated with the field ionization process is very long when $\gamma \ll \gamma_c$.

We also assume that the static electric field is small enough to neglect the deformation of the envelope function and the Stark shift. This is justified by the fact that in the quantum-defect approach the ground state is mostly determined by the short-range potential.[8] Note that this approximation becomes less valid for the hydrogenic limit since there is no short-range potential. This approximation nevertheless remains acceptable if we work with very weak fields in this case. We have verified explicitly, using a variational approach not presented here, that the envelope function deformation and the Stark shift resulting from the static field were very small for all the cases discussed in Sec. V.

If we neglect the electric field contribution, the Hamiltonian $H(\vec{r})$ reduces to the well-known quantum-defect problem. For an optical transition, the dipolar operator vanishes for $z = 0$ and the most important contribution to the matrix elements comes from outside the near-origin region [see Eq. (9)].[8] For a spherically symmetric (s-like) ground state, the quantum-defect envelope function is well known in that region and is fortunately normalizable.[13] In the hydrogenic and Lucovsky limits, the ground state is also well known. Table I gives the eigenenergy E_d and the envelope function $F_d(\vec{r})$ for the various cases. To facilitate the forthcoming developments, the envelope functions are given in the following form:

$$F_d(\vec{r}) = N_d \Phi(r) \ , \quad (4)$$

where N_d is a normalization constant and $\Phi(r)$ a spherically symmetric radial function.

C. Continuum states

Evaluating continuum extended states in the quantum-defect approach is a difficult task even in the absence of a static electric field.[8,14] In this work, we follow Bebb who neglects the impurity potential in their evaluation.[6]

In presence of an external static electric field, the continuum states are thus determined by the following Schrödinger equation:

$$(-\nabla^2 + \gamma z)F_f(\vec{r}) = E_f F_f(\vec{r}) \ . \quad (5)$$

The eigenstates are[15]

$$F_f(\vec{r}) = N_f \, e^{i(k_x x + k_y y)} \, \mathrm{Ai}\left[\gamma^{1/3}\left(z - \frac{\epsilon_z}{\gamma}\right)\right] \ , \quad (6)$$

where Ai(x) is the Airy function and N_f is a normalization constant

TABLE I. Impurity ground-state envelope functions $F_d(\vec{r}) = N_d\Phi(r)$ and related eigenenergies E_d.

Case	E_d[a]	N_d	$\Phi(r)$[b]
Quantum defect[c]	$-1/\nu^2$	$\left\{2\pi\nu\sum_{n=0}^{\infty}1/[\Gamma(-\nu)(\nu-n)(\nu-n-1)]^2\right\}^{-1/2}$	$W_{\nu,1/2}(2r/\nu)/r$
Hydrogenic	-1	$1/\sqrt{\pi}$	$\exp(-r)$
Lucovsky	$-1/\nu^2$	$1/\sqrt{2\pi\nu}$	$\exp(-r/\nu)/r$

[a] E_d is given in units of Ry*.
[b] The r variable is given in units of a_0^*.
[c] $W_{\nu,\mu}(z)$ is a Whittaker function (Ref. 18).

$$N_f = \frac{1}{2\pi\gamma^{1/6}} \ . \tag{7}$$

The eigenenergies are given by

$$E_f = k_x^2 + k_y^2 + \epsilon_z, \tag{8}$$

where k_x and k_y are the x and y components of the electron wave vector in the Brillouin zone and ϵ_z can take any value, positive or negative. Note that a more precise treatment would show that ϵ_z takes equally spaced discrete values: the so-called Wannier levels.[16] But for bulk materials, the spacing between those levels is usually small and ϵ_z can be treated as a continuous variable with a constant density of states.

The static electric field thus transforms the plane wave states of positive energy into more localized states with positive or negative energies characterized by k_x, k_y, and ϵ_z. In the following, we also use these functions when studying processes involving hydrogenic and Lucovsky ground states.

III. PHOTOIONIZATION CROSS SECTION

Using the above information concerning initial and final states, we calculate the photoionization cross section. From Fermi's golden rule, in the dipolar approximation, it can be written[9]

$$\sigma(\hbar\omega) = \frac{4\pi^2\,\alpha_0\,\hbar\omega}{n}\left(\frac{E_{\text{eff}}}{E_0}\right)^2\left(\frac{m^*}{m}\right)^2 \times \sum_f |\langle F_d(\vec{r})|\,\vec{\tau}\cdot\vec{r}\,|F_f(\vec{r})\rangle|^2\,\delta(E_f - E_d - \hbar\omega) \ , \tag{9}$$

where α_0 is the fine structure constant, $\hbar\omega$ the photon energy, $\vec{\tau}$ the electric polarization vector of the incoming photons, n the refractive index of the semiconductor, and the factors E_{eff}/E_0 and m^*/m are, respectively, the effective electric field (of the incoming light) and effective mass ratios.[9]

Calculations are performed for photons of polarization parallel or perpendicular to the static electric field (which heads in the z direction). Identifying each situation with indices z and x, respectively, we carry the calculations concurrently using $\{{}^z_x\}$ to indicate the case under consideration. In Eq. (9), we transform the summation over final states into a three-dimensional (3D) integral and rewrite the photoionization cross section as

$$\sigma_{\{{}^z_x\}}(\hbar\omega) = C\,\hbar\omega \int_{-\infty}^{+\infty}\int\!\!\int_{\text{BZ}_{xy}} |I_{\{{}^z_x\}}(k_x,k_y,\epsilon_z)|^2 \times \delta[\hbar\omega - (k_x^2 + k_y^2 + \epsilon_z - E_d)]\,dk_x\,dk_y\,d\epsilon_z \ , \tag{10}$$

where

$$C = \frac{4\pi^2\alpha_0}{n}\left(\frac{E_{\text{eff}}}{E_0}\right)^2\left(\frac{m^*}{m}\right)^2 \tag{11}$$

and

$$I_{\{{}^z_x\}}(k_x,k_y,\epsilon_z) = \int F_d^*(\vec{r})\begin{Bmatrix} z \\ x \end{Bmatrix} F_f(\vec{r})\,dr^3 \ . \tag{12}$$

The integral in $I_\alpha(k_x,k_y,\epsilon_z)$ (the index α denotes the z or x case) extends over all space. In $\sigma_\alpha(\hbar\omega)$, the integrations on k_x and k_y are performed over the projection of the Brillouin zone in the k_x-k_y plane (identified as BZ_{xy}). We approximate this projection by a circle of radius k_b. Since the integrand is a rapidly decreasing function of k_x and k_y, this simplification does not introduce a significant error.

In Appendix A, we show that each of the two 3D integrals in Eqs. (10) and (12) can be reduced to a one-dimensional form. The resulting expression for the photoionization cross section can easily be handled numerically. It is given by

$$\sigma_{\{{}^z_x\}}(\hbar\omega) = \frac{C\,\hbar\omega\,N_d^2\,N_f^2}{\pi\,\gamma^{2/3}}\begin{Bmatrix} 1 \\ \frac{1}{2} \end{Bmatrix}\int_{\hbar\omega+E_d-k_b^2}^{\hbar\omega+E_d}\left|\int_0^\infty \begin{Bmatrix} \sin\left(\frac{k_z^3}{3\gamma} - \frac{k_z\epsilon_z}{\gamma}\right) R_z[\sqrt{\hbar\omega-(\epsilon_z-E_d)},k_z] \\ \cos\left(\frac{k_z^3}{3\gamma} - \frac{k_z\epsilon_z}{\gamma}\right) R_x[\sqrt{\hbar\omega-(\epsilon_z-E_d)},k_z] \end{Bmatrix} dk_z\right|^2 d\epsilon_z \ . \tag{13}$$

The functions $R_z(k_{xy},k_z)$ and $R_x(k_{xy},k_z)$ are defined in Appendix A [Eqs. (A4a) and (A4b)]. We present below their specific expressions in the quantum-defect, hydrogenic, and Lucovsky cases. In the two latter cases, the evaluations are easily done. In the quantum-defect case, the calculations starting with the Whittaker function of Table I give complicated results. But the dipolar interaction matrix elements of the photoionization process effectively involve the envelope function outside the near origin region. Consequently, we use a standard approximation for the quantum-defect envelope function which is valid far from the origin:[6,8,9]

$$\Phi_{qd}(r) \approx \left(\frac{2r}{\nu}\right)^\nu \frac{e^{-r/\nu}}{r} \ . \tag{14}$$

The R functions are then given by ($k^2 = k_{xy}^2 + k_z^2$):
(i) hydrogenic model

$$R_{\{{}^z_x\}}(k_{xy},k_z) = -\frac{32\pi\begin{Bmatrix} k_z \\ k_{xy} \end{Bmatrix}}{(1+k^2)^3} \ ; \tag{15}$$

(ii) Lucovsky model

$$R_{\{\substack{z\\x}\}}(k_{xy},k_z)=-\frac{8\pi\left\{\begin{array}{c}k_z\\k_{xy}\end{array}\right\}}{(\frac{1}{\nu^2}+k^2)^2}\ ; \tag{16}$$

(iii) quantum-defect model

$$R_{\{\substack{z\\x}\}}(k_{xy},k_z)=C_\nu\,\nu\,\frac{\left\{\begin{array}{c}k_z\\k_{xy}\end{array}\right\}}{k}\,Z_\nu(k\nu)\ , \tag{17a}$$

with

$$C_\nu=4\pi\,2^\nu\,\nu^2\,\Gamma(\nu+1) \tag{17b}$$

and

$$\begin{aligned}Z_\nu(\rho)=&\frac{1}{\rho^2\,(1+\rho^2)^{\frac{\nu+3}{2}}}\\&\times\{-[1+(\nu+2)\rho^2]\sin[(\nu+1)\arctan(\rho)]\\&\quad+(\nu+1)\rho\cos[(\nu+1)\arctan(\rho)]\}\ .\end{aligned} \tag{17c}$$

From these equations, we have all the information necessary to compute the photoionization cross sections. Due to the nature of these expressions, numerical calculations have to be done. Before proceeding to these evaluations, we look at asymptotic limits.

IV. ASYMPTOTIC LIMITS

In this section we present asymptotic expressions for the photoionization cross section [Eq. (10)] in the limit of weak electric fields ($\hbar\omega/\gamma^{2/3}\gg 1$) for photon energies outside the neighborhood of the zero-field absorption threshold ($|\hbar\omega+E_d|/\gamma^{2/3}\gg 1$). The derivation of these expressions is outlined in Appendix B only for the z-polarization case, the treatment of the x-polarization case being similar.

In the z-polarization case, for photon energies above the zero-field absorption threshold ($\hbar\omega>|E_d|$), we obtain

$$\sigma_z(\hbar\omega)\approx\sigma_0(\hbar\omega)\left[1+\frac{3\gamma}{4\,(\hbar\omega+E_d)^{3/2}}\times\cos\left(\frac{4}{3}\frac{(\hbar\omega+E_d)^{3/2}}{\gamma}\right)\right], \tag{18}$$

where $\sigma_0(\hbar\omega)$ is the zero-field photoionization cross section defined by

$$\sigma_0(\hbar\omega)=\frac{C\,\hbar\omega\,N_d^2}{12\,\pi^2}\,(\hbar\omega+E_d)^{3/2}\,Q_1^2(\sqrt{\hbar\omega+E_d}) \tag{19}$$

and Q_1 is defined in Appendix B [Eq. (B2)]. The latter can be related to the R_z functions given in the preceding section by

$$Q_1(k_{xy})=-\lim_{k_z\to 0}R_z(k_{xy},k_z)/k_z\ . \tag{20}$$

For $\hbar\omega<|E_d|$, we obtain

$$\sigma_z(\hbar\omega)\approx C\,\hbar\omega\,\frac{N_d^2\,\gamma}{32\,\pi^2}\,Q_1^2(i\sqrt{|\hbar\omega+E_d|})\,e^{-\frac{4}{3}\frac{|\hbar\omega+E_d|^{3/2}}{\gamma}}\ . \tag{21}$$

For photon energies above $|E_d|$, Equation (18) shows that the electric field adds an oscillation pattern to the zero-field curve. Below $|E_d|$, Eq. (21) indicates that a weak static field induces an exponential redshift of the lower absorption edge.

Equation (21) can be compared with the results obtained by Coon and Karunasiri.[5] In both cases an exponential tail is found, with identical dependence on the electric field. The prefactor is, however, different. This discrepancy is related to different final state envelope functions. Coon and Karunasiri use final state wave functions that depend on the electric field and on the impurity potential. Our final state wave functions do not depend on the nature of the defect. In the Lucovsky limit, their final states are less sensitive to the impurity potential. We then find that our prefactor exhibits the same linear dependence on the electric field as in the expression given by Coon and Karunasiri for a neutral defect.[5]

Our asymptotic results are also very similar to those describing the photon-induced interband transition process in presence of a static electric field. As can be seen from the expressions of Sec. 8.4 in Ref. 15, the static field also induces oscillations and a redshift in this case (Franz-Keldysh effects). The frequency of these Franz-Keldysh oscillations is the same as in Eq. (18) if one replaces the effective mass by the reduced effective mass of the two bands involved. The exponential dependence of the redshifts shows a similar concordance. The amplitude of both effects varies linearly with the electric field for the two processes. (Note that there is a misprint in the asymptotic expression presented at the bottom of p. 272 of Ref. 15. There should be a $\theta_f^{3/2}$ dependence of the prefactor instead of the reported $\theta_f^{1/2}$ dependence.)

Similar expressions can be derived for the x-polarization case. For $\hbar\omega<|E_d|$, we find

$$\sigma_x(\hbar\omega)\approx C\,\hbar\omega\,\frac{N_d^2\,\gamma^2}{128\,\pi^2}\,\frac{Q_1^2(i\sqrt{|\hbar\omega+E_d|})}{|\hbar\omega+E_d|^{3/2}}\,e^{-\frac{4}{3}\frac{|\hbar\omega+E_d|^{3/2}}{\gamma}} \tag{22}$$

and for $\hbar\omega>|E_d|$

$$\sigma_x(\hbar\omega)\approx\sigma_0(\hbar\omega)\left(1+\frac{\gamma^2}{(\hbar\omega+E_d)^3}\,\tau(\hbar\omega,E_d,\gamma)\right), \tag{23}$$

where $\tau(\hbar\omega,E_d,\gamma)$ contains an oscillating function, the amplitude of the oscillations being independent of γ. We obtain again an oscillation pattern and a redshift. But the amplitude of these effects is of the order of $\gamma/|\hbar\omega+E_d|^{3/2}$ smaller than it is in the z-polarization case. For example, in the next section, we consider a defect of ground-state energy $E_d=-4$ Ry* in the presence of a static electric field characterized by $\gamma=0.1$. For these values, we expect that the above effects (oscillations for $\hbar\omega>|E_d|$ and exponential tail for $\hbar\omega<|E_d|$) in the x-polarization case should be of the order of 80

times smaller than for those found in the z-polarization case.

V. NUMERICAL RESULTS

To illustrate our formalism, we consider a moderately deep impurity level of energy $E_d = -4\,\mathrm{Ry}^*$ ($\nu = 0.5$) and a deep one of energy $E_d = -69.5\,\mathrm{Ry}^*$ ($\nu = 0.12$). We evaluate the photoionization cross sections for static electric-field magnitudes such that $\gamma = \gamma_c/10$ and $\gamma = \gamma_c/20$ [γ_c is defined in Eq. (3)] in order to neglect field ionization processes. This gives γ values of 0.2 and 0.1 for the $-4\,\mathrm{Ry}^*$ level and of 60.3 and 30.1 for the $-69.5\,\mathrm{Ry}^*$ level. Using GaAs parameters[17] ($a_0^* = 104$ Å, $\mathrm{Ry}^* = 5.39$ meV), the above parameters would correspond to a shallow level of 21.6 meV and a deep level of 375 meV. For the shallow level, the applied electric fields would then be 1.04×10^3 V/cm and 5.2×10^2 V/cm and for the deep level, 3.14×10^5 V/cm and 1.57×10^5 V/cm.

From the asymptotic expressions of the last section, we see that the magnitude of the oscillations is proportional to the ratio $\gamma/|\hbar\omega + E_d|^{3/2}$ in the z-polarization case. Our evaluated cross sections are of interest for photon energies of the order of $|E_d|$. Consequently, the ratio $\gamma/|E_d|^{3/2}$ gives a rough estimate of the magnitude of these oscillations. The limiting ratio $\gamma_c/|E_d|^{3/2} = 1/(8\nu)$ is smaller for a shallow defect than for a deep one, we thus expect to see larger effects for the deep $-69.5\,\mathrm{Ry}^*$ impurity level than for the $-4\,\mathrm{Ry}^*$ one.

We first present photoionization cross sections based on the quantum-defect model. They are given in Figs. 1 ($-4\,\mathrm{Ry}^*$ defect) and 2 ($-69.5\,\mathrm{Ry}^*$ defect) for the z and x polarizations of the incoming photon flux. For comparison, we have also presented the zero-field cross sections. The results for the z and x polarizations are different and require a separate discussion.

In the z-polarization case [Figs. 1(a) and 2(a)], our calculated photoionization curves agree very well with the behavior suggested by the asymptotic expressions of the previous section: appearance of a redshift of the lower absorption edge and superimposition of oscillations on the zero-field curve. As indicated by the electric-field dependence of Eq. (18), the period and the amplitude of these oscillations increase with the magnitude of the applied static electric field. Their amplitude decreases as the photon energy increases. Their period is not constant but also decreases with an increase in photon energy as shown by the $(\hbar\omega + E_d)^{3/2}$ dependence of the oscillating term of Eq. (18). Our asymptotic expression indicates that the oscillation period should vary with the electric field as $\gamma^{2/3}$. This behavior is verified by our calculated cross sections. In Fig. 3, we compare the asymptotic cross sections [Eq. (21)] for $\hbar\omega < |E_d|$ and Eq. (18) for $\hbar\omega > |E_d|$) with the calculated one for the $-4\,\mathrm{Ry}^*$ level with $\gamma = 0.1$. One can see that the agreement is nearly perfect outside the neighborhood of the zero-field absorption threshold. Note that the two asymptotic expressions have different values when $\hbar\omega = |E_d|$, resulting in a mismatch between the curves at that point.

In the x-polarization case [Figs. 1(b) and 2(b)], the effects are much smaller and almost negligible except for very strong fields. This was already suggested by the asymptotic expressions of Eqs. (22) and (23) where the effects were of much smaller amplitude than in the z-polarization case. Physically this is reasonable since the static electric field mostly deforms the final extended states along the z direction. Consequently, the dipolar matrix element of Eq. (9) is much less affected by this deformation in the x-polarization case than it is in the z-polarization case.

Although not presented here, we have performed calculations based on the Lucovsky approach for the same parameters as above. This approach corresponds to the omission of the Coulombic part of the impurity potential and the results should be identical to the quantum-defect ones for an extremely deep impurity level ($\nu \ll 1$). For the defect energy considered, the zero-field cross section takes smaller values in the Lucovsky case since the ground-state envelope function is more localized. But the

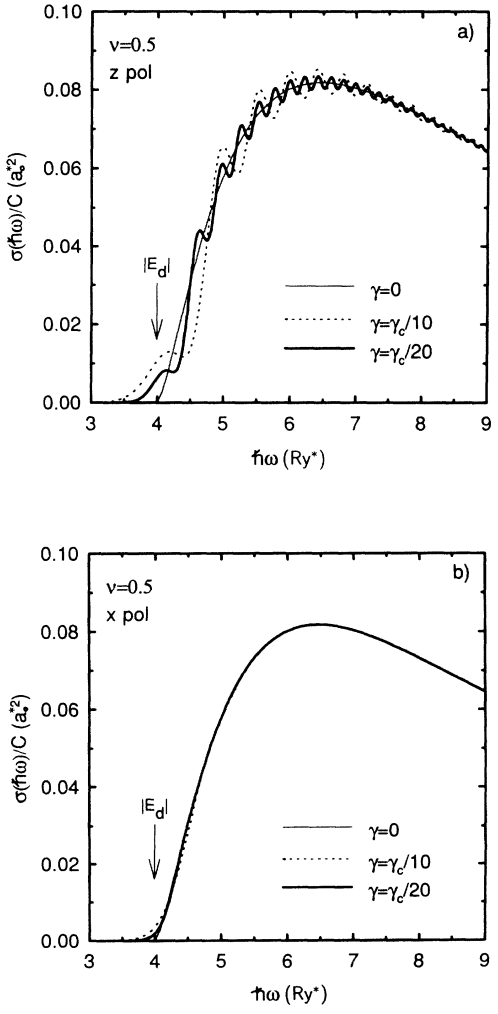

FIG. 1. Photoionization cross sections for the quantum-defect model of the impurity potential with $\nu = 0.5$ (a) in the z-polarization case and (b) in the x-polarization case. As an example, for GaAs, a value of 0.1 corresponds to a cross section of 0.372×10^{-16} cm^2.

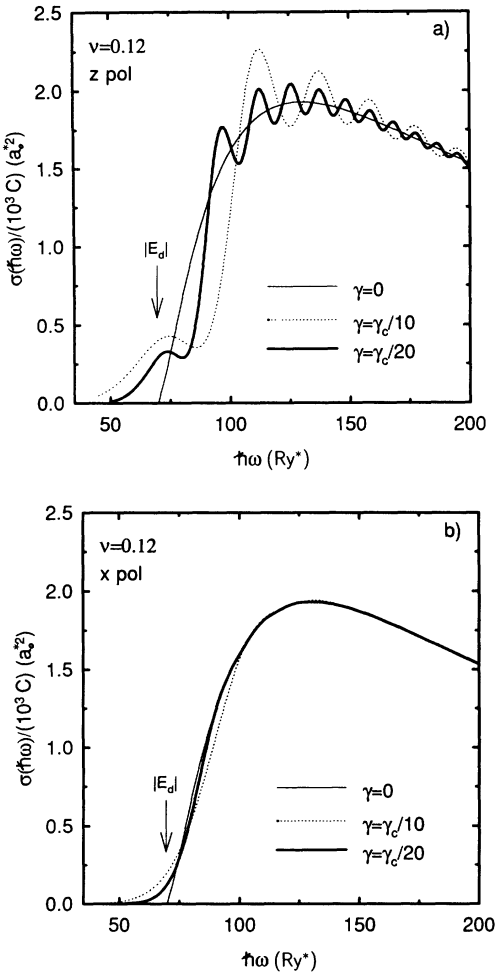

FIG. 2. Photoionization cross sections for the quantum-defect model of the impurity potential with $\nu = 0.12$ (a) in the z-polarization case and (b) in the x-polarization case. As an example, for GaAs, a value of 2.5 corresponds to a cross section of 9.3×10^{-16} cm^2.

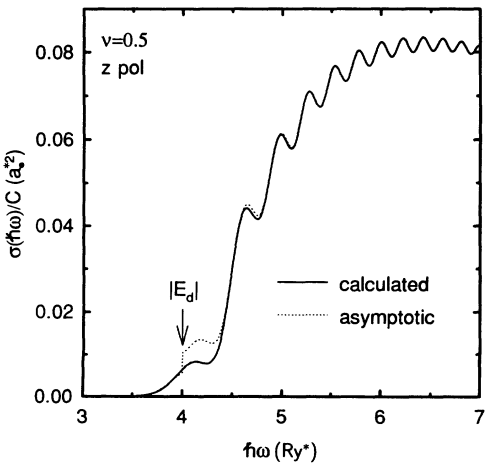

FIG. 3. Comparison between asymptotic (see text) and calculated cross sections for $\nu = 0.5$ and $\gamma = 0.1$ in the z-polarization case.

qualitative aspects of the static field effects are the same as above: oscillations and redshift in the z-polarization case and almost no effect in the x-polarization case. Compared to the quantum-defect curves, the oscillation periods are identical for similar γ values. This is a consequence of the fact that the oscillation periods are fixed by the nature of the final extended states which are the same in both cases.

Finally, photoionization cross section curves based on the hydrogenic model have also been calculated. They are not presented here since the effects of the static electric field on the photoionization cross section are similar to those described above.

VI. CONCLUSION

In this paper, we have studied the photoionization process of an isolated semiconductor impurity in the presence of a static uniform electric field. The magnitude of the latter is kept well below the classical field ionization threshold.

We find that the main effects of the electric field are the superimposition of oscillations on the zero-field photoionization curve and the appearance of a redshift of the lower absorption edge. The order of magnitude and the general behavior of the photoionization cross sections are however unchanged when an electric field is added. Our calculations show that these effects are much weaker when the polarization of the incident photon flux is perpendicular to the electric field (x-polarization case) than when the polarization is along the electric field (z-polarization case). For the parallel configuration, the asymptotic expression shows that the oscillations have a period which depends on the electric field $E_{\rm el}$ as $E_{\rm el}^{2/3}$. Those considerations are similar to the Franz-Keldysh effects related to the photon-induced interband transition process in presence of a static electric field.

These effects have not yet, to our knowledge, been observed experimentally in the case of a defect. As an example, DLOS measurements do not exhibit such a behavior. The main reason for this is that the perpendicular configuration (x-polarization case) is used in these types of measurements. In this case, the oscillations are predicted to be very weak for reasonable values of electric fields. Also, in a junction, the electric field is usually not uniform: it varies across the depletion region. As a consequence, the weak oscillation pattern is smeared out by the electric field variation.

In order to observe the above oscillations, a coplanar configuration should be used. A uniform electric field should be applied parallel to the surface of the sample. The incoming photon should be polarized in the direction of the static field. In this case, oscillations would be seen for large enough electric fields in optical absorption or in photoconductivity measurements. The effect is predicted to be easier to observe for a deep defect, since higher electric fields can be applied without ionizing the impurity.

The above theoretical treatment has been carried on neglecting the electron-phonon interaction. This interac-

tion is known to be strong in polar crystals and weak in covalent semiconductors. Consequently, we expect this effect to be small in Si, Ge, or in III-V compounds. Also of interest to improve the above calculations are better wave functions for the initial and final states. These improvements would help to extend the range of applicability of our treatment.

ACKNOWLEDGMENTS

This research has been supported by the Natural Science and Engineering Research Council of Canada (NSERC) and by le Ministère de l'Éducation du Québec [le Fonds pour la Formation de Chercheurs et l'Aide à la Recherche (FCAR)]. We would also like to thank E. Kartheuser for stimulating discussions concerning the quantum-defect model.

APPENDIX A

In this appendix, we show how each of the three-dimensional integrals appearing in the definitions of $I_\alpha(k_x,k_y,\epsilon_z)$ [Eq. (12)] and of $\sigma(\hbar\omega)$ [Eq. (10)] can be reduced to one dimension.

Using the following integral representation of the Airy function,[15]

$$\mathrm{Ai}(\xi)=\frac{1}{2\pi}\int_{-\infty}^{\infty} e^{i\left(\frac{t^3}{3}+t\,\xi\right)}\,dt\ , \tag{A1}$$

we rewrite the final state envelope functions [Eq. (6)] as ($t=k_z/\gamma^{1/3}$):

$$F_f(\vec{r})=\frac{N_f}{2\pi\gamma^{1/3}}\int_{-\infty}^{+\infty} e^{i\left(\frac{k_z^3}{3\gamma}-\frac{k_z\epsilon_z}{\gamma}\right)}\,e^{i\vec{k}\cdot\vec{r}}\,dk_z\ . \tag{A2}$$

Introducing this expression along with $F_d(\vec{r})$ [Eq. (4)] in the definition of $I_\alpha(k_x,k_y,\epsilon_z)$ [Eq. (12)], one can easily get

$$I_{\{\substack{z\\x}\}}(k_x,k_y,\epsilon_z)=\frac{N_dN_f}{2\pi\gamma^{1/3}}\int_{-\infty}^{+\infty} e^{i\left(\frac{k_z^3}{3\gamma}-\frac{k_z\epsilon_z}{\gamma}\right)} \times(-i)\begin{Bmatrix} R_z(k_{xy},k_z)\\ \cos(\phi)\,R_x(k_{xy},k_z)\end{Bmatrix} dk_z\ , \tag{A3}$$

where $k_{xy}=\sqrt{k_x^2+k_y^2}$, ϕ is a polar angle defined in the k_x-k_y plane such that $k_x=k_{xy}\cos(\phi)$ and the $R_z(k_{xy},k_z)$ and $R_x(k_{xy},k_z)$ functions are defined by

$$R_z(k_{xy},k_z)=\frac{\partial}{\partial k_z}\int\Phi(r)\,e^{i\vec{k}\cdot\vec{r}}\,dr^3\ , \tag{A4a}$$

$$R_x(k_{xy},k_z)=\frac{\partial}{\partial k_{xy}}\int\Phi(r)\,e^{i\vec{k}\cdot\vec{r}}\,dr^3\ . \tag{A4b}$$

Now, using the parity of $R_z(k_{xy},k_z)$ and $R_x(k_{xy},k_z)$ we can rewrite

$$I_{\{\substack{z\\x}\}}(k_x,k_y,\epsilon_z)=\frac{N_dN_f}{\pi\gamma^{1/3}}\int_0^{+\infty}\begin{Bmatrix}\sin\left(\frac{k_z^3}{3\gamma}-\frac{k_z\epsilon_z}{\gamma}\right)R_z(k_{xy},k_z)\\ (-i)\cos(\phi)\cos\left(\frac{k_z^3}{3\gamma}-\frac{k_z\epsilon_z}{\gamma}\right)R_x(k_{xy},k_z)\end{Bmatrix}dk_z\ . \tag{A5}$$

Since the R functions can be evaluated analytically for the three models of the impurity potential, we have reduced the three-dimensional integral appearing in the expression of $I_\alpha(k_x,k_y,\epsilon_z)$ to a one-dimensional form that can be easily evaluated numerically, except for very small values of γ.

Now, introducing Eq. [A5] into the definition of $\sigma(\hbar\omega)$ [Eq. (10)], one can easily perform the integration over the k_x-k_y plane. It is done by taking into account the polar symmetry of the $R_z(k_{xy},k_z)$ and $R_x(k_{xy},k_z)$ functions in this plane. One then obtains Eq. (13).

APPENDIX B

In this appendix, we derive the asymptotic expressions of Sec. IV for the z-polarization case. These expressions are valid for weak electric fields and for photon energies far from the zero-field absorption threshold. We first expand the Airy function of the final state in Eq. (12) around $z=0$ to get

$$I_z(k_x,k_y,\epsilon_z)=N_dN_f\sum_{n\,\mathrm{odd}} \times Ai^{(n)}\left(-\frac{\epsilon_z}{\gamma^{2/3}}\right)\frac{\gamma^{n/3}}{n!}Q_n(k_{xy})\ , \tag{B1}$$

where

$$Q_n(k_{xy})=\int\Phi(r)\,z^{n+1}e^{i(k_xx+k_yy)}\,dr^3 \tag{B2}$$

and $\mathrm{Ai}^{(n)}(x)$ is the nth derivative of the Airy function. Due to the radial symmetry of the $\Phi(r)$'s considered, the integral defining $Q_n(k_{xy})$ only depends on k_x and k_y through $k_{xy}=\sqrt{k_x^2+k_y^2}$. Although defined for real positive values of k_{xy}, the functions $Q_n(k_{xy})$ can be extended to imaginary arguments. The resulting functions are real valued.

Substituting Eq. (B1) in Eq. (10), we approximate the projection of the Brillouin zone in the k_x-k_y plane by a

circle of radius k_b. Using the radial symmetry of $Q_n(k_{xy})$ in this plane, we integrate over k_x and k_y to get

$$\sigma_z(\hbar\omega) = C\,\hbar\omega\,N_d^2\,N_f^2\,\pi \times \int_{(\hbar\omega+E_d-k_b^2)}^{\hbar\omega+E_d} \left[\sum_{n\ \mathrm{odd}} \mathrm{Ai}^{(n)}\left(-\frac{\epsilon_z}{\gamma^{2/3}}\right)\frac{\gamma^{n/3}}{n!} \times Q_n(\sqrt{\hbar\omega+E_d-\epsilon_z})\right]^2 d\epsilon_z \ . \quad \text{(B3)}$$

For weak electric fields, the integrand rapidly decreases for negative values of ϵ_z. In the context of the effective-mass approximation, $\hbar\omega + E_d - k_b^2 < 0$ and the lower bound can be extended to $-\infty$. We develop the integrand and make the change of variable $u = -\epsilon_z/\gamma^{2/3}$ to get

$$\sigma_z(\hbar\omega) = C\,\hbar\omega\,N_d^2\,N_f^2\,\pi\,\gamma^{2/3} \times \sum_{n,m\ \mathrm{odd}} \int_{-\frac{(\hbar\omega+E_d)}{\gamma^{2/3}}}^{+\infty} \mathrm{Ai}^{(n)}(u)\,\mathrm{Ai}^{(m)}(u) \times \frac{\gamma^{(n+m)/3}}{n!\,m!} Q_n(\sqrt{\hbar\omega+E_d+\gamma^{2/3}u}) \times Q_m(\sqrt{\hbar\omega+E_d+\gamma^{2/3}u})\,du \ . \quad \text{(B4)}$$

We expand the integrand around $u = 0$, leaving the Airy functions unchanged. One can verify that, for the $\Phi(r)$'s considered, the term with $n = 1$ and $m = 1$ gives the main contribution in the limits $\hbar\omega/\gamma^{2/3} \gg 1$ (weak electric field) and $|\hbar\omega + E_d|/\gamma^{2/3} \gg 1$ (photon energy outside the region of the zero-field absorption threshold). Using asymptotic expansions of the integral

$$\int_a^\infty \mathrm{Ai}'^2(u)du = \frac{1}{3}[-a\mathrm{Ai}'^2(a) + a^2\mathrm{Ai}^2(a) - 2\mathrm{Ai}'(a)\mathrm{Ai}(a)] \ , \quad \text{(B5)}$$

Eqs. (18) and (21) can be easily obtained.

[1] G.F. Neumark and K. Kosai, in *Semiconductors and Semimetals*, edited by R.K. Willardson and A.C. Beer (Academic Press, New York, 1983), Vol. 19, p. 1.
[2] A. Chantre, D. Vincent, and D. Bois, Phys. Rev. B **23**, 5335 (1981).
[3] J.L. Pautrat, Solid-State Electron. **23**, 661 (1980).
[4] B. Monemar and L. Samuelson, Phys. Rev. B **18**, 809 (1978).
[5] D.D. Coon and R.P.G. Karunasiri, Solid-State Electron. **26**, 1151 (1983).
[6] H. Barry Bebb, Phys. Rev. **185**, 1116 (1969).
[7] F.S. Ham, Solid State Physics **1**, 127 (1955).
[8] H. Barry Bebb and R.A. Chapman, J. Phys. Chem. Solids **28**, 2087 (1967).
[9] S. Chaudhuri, Phys. Rev. B **26**, 6593 (1982).
[10] S.T. Pantelides, Rev. Mod. Phys. **50**, 797 (1978).
[11] G. Lucovsky, Solid State Commun. **3**, 299 (1965).
[12] J.E. Bayfield, Phys. Rep. **51**, 317 (1979).
[13] S. Chaudhuri, D.D. Coon, and G.E. Derkits, Phys. Rev. A **23**, 1657 (1981).
[14] M.J. Seaton, Mon. Not. R. Astron. Soc. **118**, 504 (1958).
[15] F. Bassani and G.P. Parravicini, *Electronic States and Optical Transitions in Solids* (Pergamon, Oxford, 1975).
[16] J. Callaway, *Quantum Theory of the Solid State* (Academic Press, San Diego, 1974).
[17] E. Kartheuser, in *Polarons in Ionic Crystals and Polar Semiconductors*, edited by J.T. Devreese (North-Holland, Amsterdam, 1972), p. 717.
[18] *Handbook of Mathematical Functions*, edited by M. Abramowitz and I.A. Stegun (Dover, New York, 1965).